© 2020. Published by The Company of Biologists Ltd | Journal of Experimental Biology (2020) 223, jeb223776. doi:10.1242/jeb.223776

RESEARCH ARTICLE

Stable mitochondrial $CICIII_2$ supercomplex interactions in reptiles versus homeothermic vertebrates

Amanda Bundgaard[1,‡], Andrew M. James[2], Michael E. Harbour[2], Michael P. Murphy[2,*] and Angela Fago[1,*]

ABSTRACT

The association of complex I (CI), complex III (CIII) and complex IV (CIV) of the mitochondrial electron transport chain into stable high molecular weight supercomplexes (SCs) has been observed in several prokaryotes and eukaryotes, but among vertebrates it has only been examined in mammals. The biological role of these SCs is unclear but suggestions so far include enhanced electron transfer between complexes, decreased production of the reactive oxygen species (ROS) O_2^- and H_2O_2, or enhanced structural stability. Here, we provide the first overview on the stability, composition and activity of mitochondrial SCs in representative species of several vertebrate classes to determine patterns of SC variation across endotherms and ectotherms. We found that the stability of the $CICIII_2$ SC and the inclusion of CIV within the SC varied considerably. Specifically, when solubilized by the detergent DDM, mitochondrial $CICIII_2$ SCs were unstable in endotherms (birds and mammals) and highly stable in reptiles. Using mass-spectrometric complexomics, we confirmed that the $CICIII_2$ is the major SC in the turtle, and that 90% of CI is found in this highly stable SC. Interestingly, the presence of stable SCs did not prevent mitochondrial H_2O_2 production and was not associated with elevated respiration rates of mitochondria isolated from the examined species. Together, these data show that SC stability varies among vertebrates and is greatest in poikilothermic reptiles and weakest in endotherms. This pattern suggests an adaptive role of SCs to varying body temperature, but not necessarily a direct effect on electron transfer or in the prevention of ROS production.

KEY WORDS: Bioenergetics, Complexomics, Mass spectrometry, Mitochondria, Oxidative phosphorylation, Reactive oxygen species

INTRODUCTION

The electron transport chain (ETC) in the mitochondrial inner membrane has classically been viewed as a series of four individual large membrane protein complexes (CI–CIV). These complexes transfer electrons delivered by NADH to complex I (CI, NADH dehydrogenase) or by succinate to complex II (CII, succinate dehydrogenase) on to complex III (CIII, ubiquinone cytochrome *c* oxidoreductase) by reducing ubiquinone to ubiquinol. Electrons are then transferred from CIII to complex IV (CIV, cytochrome *c* oxidase) via cytochrome *c*. This electron transfer is coupled to proton pumping at CI, CIII and CIV across the mitochondrial inner membrane. The resulting proton motive force drives ATP production at complex V (CV, ATP synthase). Recently, this 'fluid model' of electron transport based on diffusion-controlled, transient interactions between complexes has been challenged by the discovery of stable supercomplex (SC) associations of respiratory complexes (Schägger and Pfeiffer, 2001; Schägger et al., 2000). Typically, these SCs consist of CI and CIII, with $CICIII_2$ and CI_2CIII_2 stoichiometries, with or without CIV. SCs have been demonstrated *in vitro* using blue native polyacrylamide gel electrophoresis (BN-PAGE) (Schägger et al., 2000), by cryogenic electron microscopy (cryo-EM) of isolated SCs (Gu et al., 2016; Guo et al., 2017; Letts et al., 2016, 2019; Wu et al., 2016) and by *in situ* tomography of mitochondrial membranes (Davies et al., 2011, 2018).

While the existence of mitochondrial SCs is well established, their functional relevance is less clear. The close association of ETC complexes in SCs has been proposed to favour more efficient electron transport, potentially increasing respiration rate and decreasing electron leak and production of reactive oxygen species (ROS) products superoxide (O_2^-) and hydrogen peroxide (H_2O_2) (Acín-Pérez et al., 2008; Althoff et al., 2011; Genova and Lenaz, 2014; Greggio et al., 2016; Lapuente-Brun et al., 2013; Letts and Sazanov, 2017; Lopez-Fabuel et al., 2016; Maranzana et al., 2013; Sousa et al., 2016). This view is supported by studies in bovine, human and mouse mitochondria, where a higher degree of SC prevalence has been found to correlate with a more efficient respiration rate (Genova et al., 2008; Greggio et al., 2016; Lapuente-Brun et al., 2013) and decreased formation of O_2^- and H_2O_2 (Lopez-Fabuel et al., 2016; Maranzana et al., 2013). Alternative functions of SCs have been suggested, such as aiding correct subunit assembly of the large individual complexes, in particular CI (Milenkovic et al., 2017; Moreno-Lastres et al., 2012; Schägger et al., 2004), or preventing protein aggregation in the protein-rich mitochondrial inner membrane (Blaza et al., 2014; Milenkovic et al., 2017).

SCs have been observed when using the gentle detergent digitonin to solubilise membranes in bacteria (Gong et al., 2018; Stroh et al., 2004), yeast (Schägger et al., 2000), plants (Bultema et al., 2009; Davies et al., 2018; Eubel et al., 2004; Senkler et al., 2018), insects (Shimada et al., 2018) and, among vertebrates, in six mammalian species (Althoff et al., 2011; Davies et al., 2018; Gu et al., 2016; Letts et al., 2016, 2019; Schägger et al., 2000; Wu et al., 2016). SCs are generally readily separated into their individual complexes by the stronger detergent dodecylmaltoside (DDM), with only one reported exception, the ectothermic red-eared slider turtle *Trachemys scripta*, in which SCs are stable in the presence of DDM (Bundgaard et al., 2018). These effects of detergents indicate that lipid composition may play a role in SC formation and stability. The phospholipid cardiolipin, which is only found in the mitochondrial inner membrane in eukaryotes, stabilises individual complexes as well as SC interactions (Mileykovskaya and Dowhan, 2009, 2014; Paradies et al., 2014; Pfeiffer et al., 2003; Zhang et al.,

[1]Department of Biology, Aarhus University, 8000 Aarhus, Denmark. [2]MRC Mitochondrial Biology Unit, University of Cambridge, Cambridge CB2 0XY, UK.
*These authors contributed equally to this work

[‡]Author for correspondence (ammagabu@yahoo.dk)

A.B., 0000-0001-9716-8333; M.E.H., 0000-0003-4775-9682; M.P.M., 0000-0003-1115-9618; A.F., 0000-0001-7315-2628

Received 21 February 2020; Accepted 5 May 2020

Journal of Experimental Biology (2020) 223, jeb223776. doi:10.1242/jeb.223776

2002), whereas phosphotidylethanolamine, a component of all biological membranes, destabilises them (Böttinger et al., 2012).

Although SCs are widespread, they have been studied primarily in mammals and their occurrence, distribution and stability in other vertebrate classes has not yet been examined systematically (Acín-Pérez et al., 2008; Greggio et al., 2016; Lapuente-Brun et al., 2013; Lopez-Fabuel et al., 2016; Maranzana et al., 2013). Widening this perspective to other vertebrate species with different metabolic requirements, ranges of body temperature, rates of body temperature change and tolerance to hypoxia offers a useful approach to identify fundamental patterns of SC formation and evolution, and from this to infer some general functional roles.

Here, we analysed the occurrence of SCs in heart mitochondria from species representing major vertebrate classes to assess the abundance and pattern of SC stability, and determined which complexes comprise the DDM-insoluble highly stable turtle SC. We also related SC stability to respiration rates and production of H_2O_2 measured in isolated mitochondria. This first comparative overview of SCs offers a new perspective on the biological and evolutionary significance of mitochondrial SCs.

MATERIALS AND METHODS

Chemicals

Amplex UltraRed was purchased from ThermoFisher Scientific. All other chemicals were purchased from Sigma-Aldrich.

Animals

Animals were kept at the animal facility at Zoophysiology, Department of Biology, Aarhus University. All animals were obtained as adults from authorised vendors. The vertebrate species selected included endotherms and ectotherms (see Fig. 1A) covering a broad range of ecological body temperatures from 0 to 42°C: Wistar rat, *Rattus norvegicus* (*N*=5), zebra finch, *Taeniopygia guttata* (*N*=5), red-eared slider turtle, *Trachemys scripta elegans* (*N*=5), ball python, *Python regius* (*N*=5), bearded dragon *Pogona vitticeps* (*N*=5), African clawed frog, *Xenopus laevis* (hereafter *Xenopus*; *N*=5), crucian carp, *Carassius carassius* (*N*=5) and rainbow trout, *Oncorhynchus mykiss* (*N*=6). Rats were killed by cervical dislocation and fish were killed by a blow to the head and destruction of the brain. *Xenopus* were anaesthetised by submersion in 0.5% benzocaine before destruction of the brain. All other animals were killed by intravascular injection with an overdose (50 mg ml^{-1}) of pentobarbital and when the corneal reflex was gone they were beheaded and the brain destroyed. All animal procedures were performed according to the Danish Law on Animal Experiments.

Mitochondrial isolation

Mitochondria were isolated using the same protocol for all species to make comparisons of SC stability possible. Whole hearts (rat and zebra finch) or heart ventricles (turtles, pythons, bearded dragon, *Xenopus*, crucian carp and trout) were used for mitochondrial isolation and rinsed in ice-cold STE buffer (250 mmol l^{-1} sucrose, 5 mmol l^{-1} Tris, 1 mmol l^{-1} EGTA, pH 7.2) with 2.5% (w/v) fatty acid-free bovine serum albumin (BSA). Mitochondria were isolated by differential centrifugation as previously described (Bundgaard et al., 2018). The final mitochondrial pellet was resuspended in ∼200 µl STE buffer and a portion was immediately frozen in liquid nitrogen and stored at −80°C for analysis of SCs by BN-PAGE (see below). The remaining portion was kept on ice before respiration rate and H_2O_2 production measurements. Protein content was measured using the Pierce 660 nm protein assay using BSA as a standard.

BN-PAGE

Frozen mitochondria were thawed on ice and centrifuged at 16,000 ***g*** for 2 min. The pellet was resuspended in extraction buffer (0.75 mol l^{-1} aminocaproic acid, 50 mmol l^{-1} BisTris, pH 7.0 at 4°C) and incubated on ice with the detergent DDM (3.5 g g^{-1} mitochondrial protein) for 30 min or the more gentle detergent digitonin (6 g g^{-1} mitochondrial protein) for 15 min (Letts et al., 2016; Schägger et al., 2000). These detergent concentrations were found to consistently solubilise mitochondrial membrane proteins from both endothermic (rat) and ectothermic (turtle) species (Fig. S1). Insoluble material was pelleted by centrifugation at 13,000 ***g*** for 30 min at 4°C and solubilised membrane proteins were separated by BN-PAGE as previously described (Bundgaard et al., 2018). Size of complexes was estimated from an exponential fit to the migration distance on the gel (R^2=0.9993), determined from the approximate molecular mass of rat mitochondrial complexes: CI 880 kDa, CV 600 kDa, $CIII_2$ 460 kDa, CIV 200 kDa, CII 140 kDa (Letts et al., 2016). The distribution of complexes and SCs on BN-PAGE was assessed at least in triplicate for each species.

In-gel activity assays

To assess in-gel CIV activity, the BN-PAGE gel was incubated with 1 mg ml^{-1} cytochrome *c* (bovine), 0.5 mg ml^{-1} 3,3′-diaminobenzidine in 25 mmol l^{-1} KH_2PO_4 pH 7.4 for 40 min, and CIV activity was detected as a brown staining of bands. CI activity was assayed by incubating the gel with 1 mg ml^{-1} nitroblue tetrazolium and 0.1 mmol l^{-1} NADH for 10 min and was detected as a purple staining of bands (Greggio et al., 2016).

Complexome profiling

To determine which individual complexes are present in turtle and rat SCs, we performed profile analyses of mitochondrial membrane proteins after separation by BN-PAGE with 3.5 g DDM g^{-1} protein as described above, following the method described in Heide et al. (2012). Each BN-PAGE lane was cut into 64×1 mm equally sized slices and proteins were digested in the gel with trypsin [12.5 ng $µl^{-1}$ trypsin in 20 mmol l^{-1} Tris-HCl (pH 8) with 5 mmol l^{-1} $CaCl_2$]. Peptides were extracted from gel slices by the addition of 60% acetonitrile and 4% formic acid, and a portion of each peptide mixture was dried down and resuspended in 2% acetonitrile and 0.1% formic acid. The peptides in each gel slice were analysed sequentially using fractionation on a C18 reverse-phase Biosphere column (75 µm×150 mm; Nanoseparations, Nieuwkoop, The Netherlands) with a gradient of 5–40% acetonitrile in 0.1% formic acid at a flow rate of 300 nl min^{-1} in 84 min using Proxeon EasyLC II nanoscale liquid chromatograph and detection by a Thermo Scientific LTQ Orbitrap XL mass spectrometer (LC/MS), with fragmentation performed by collision-induced dissociation using nitrogen. For peptide sequence assignment, Proteome Discoverer (Thermo Scientific) and Mascot 2.4 (Matrix Science Ltd) software were used to compare mass spectra with NCBI databases (https://www.ncbi.nlm.nih.gov/) for *Chrysemys picta bellii*, a species closely related to *T. scripta*, and *R. norvegicus*. Search parameters included the variable peptide modifications methionine oxidation and propionamide derivatisation of cysteine, allowing the presence of only one missed cleavage, a peptide mass tolerance of 10 ppm and a fragment ion mass tolerance of 0.5 Da. The abundance of all the well-assigned peptides observed in all the samples was summed by Proteome Discoverer and its standard aggregation algorithm was used as a measure of relative protein abundance for each protein for each gel slice; up to the three highest intensity peptides for each protein were selected and averaged. A custom R script was written and used to create relative abundance profiles across the BN-PAGE lanes and to

Journal of Experimental Biology (2020) 223, jeb223776. doi:10.1242/jeb.223776

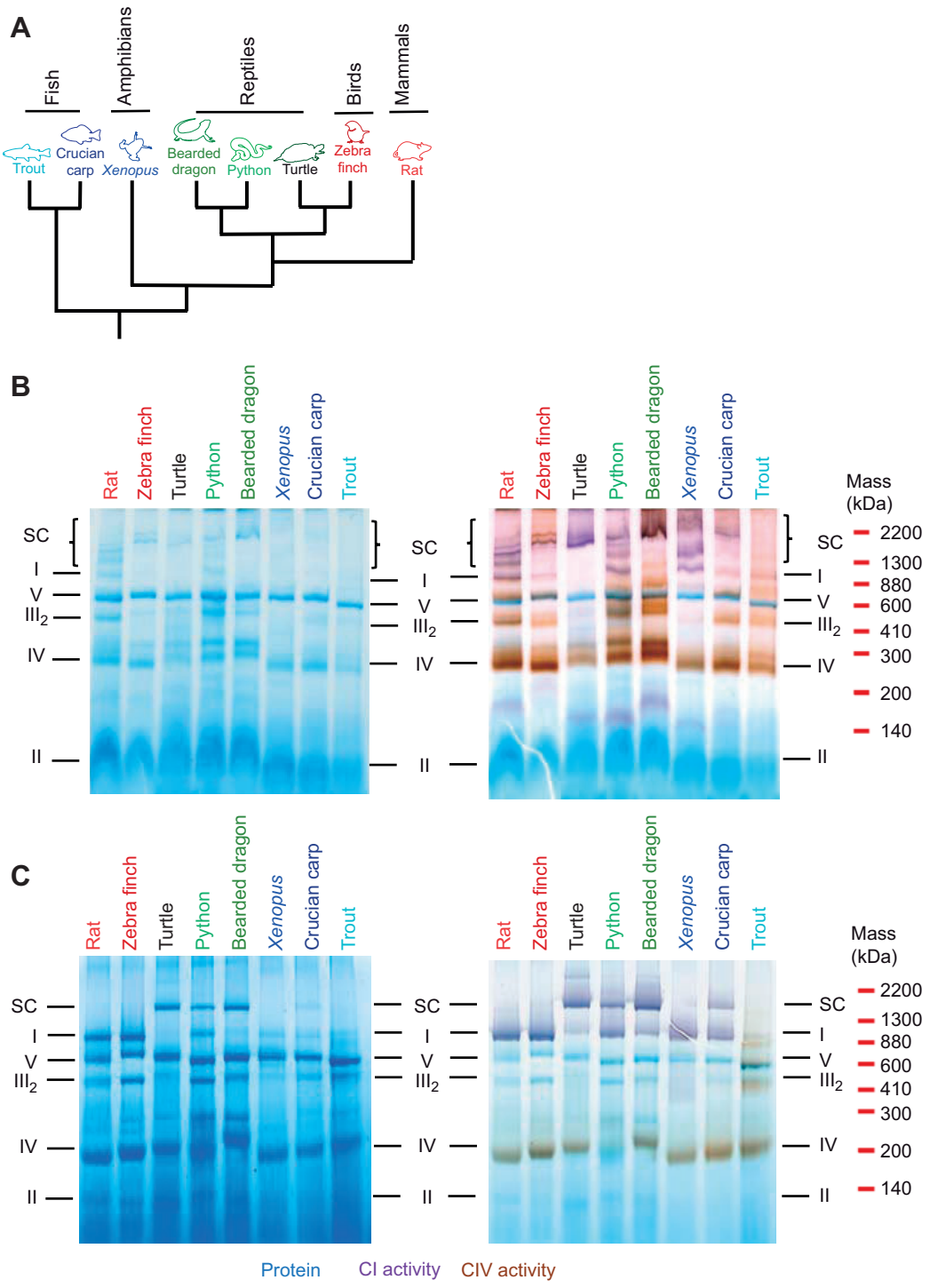

Fig. 1. Resolution of mitochondrial respiratory complexes. (A) Phylogenetic tree of the species used based on Green et al. (2014). Branch lengths do not reflect evolutionary distances between groups. (B,C) Resolution of electron transport chain (ETC) complexes by BN-PAGE from vertebrate heart mitochondria solubilised with digitonin (B) or DDM (C). The gels were stained for protein (blue), complex I (CI) activity (purple) and complex V (CIV) activity (brown). The distribution of complexes is representative of at least three independent assessments for each species. SC, supercomplex.

perform hierarchical clustering on them. A Microsoft Excel macro was written and used to create coloured visual representations (‘heatmaps’) of the profiles, which are shown in Table S1.

Enzyme assays

The enzyme assays were conducted in the presence of 0.05% DDM to permeabilise intact mitochondria, allowing access to the matrix side of the membrane proteins. All enzyme assays were conducted at 25°C on a microplate reader (Molecular Devices, San Jose, CA, USA).

CI NADH:ubiquinone activity

CI activity of the entire enzyme was assayed as the rotenone-sensitive decrease in NADH, measured as the difference in

Journal of Experimental Biology (2020) 223, jeb223776. doi:10.1242/jeb.223776

absorbance at 340 and 380 nm using an extinction coefficient ε of 6.22 l mmol^{-1} cm^{-1} (Estornell et al., 1993) based on the assay by Trounce et al. (1996). Mitochondria (5–30 µg protein per well) were added to buffer (25 mmol l^{-1} KH_2PO_4, pH 7.8) with 0.2 mmol l^{-1} KCN, 300 nmol l^{-1} antimycin A, 0.05% DDM and 0.1 mmol l^{-1} decylubiquinone as electron acceptor, and assays were initiated by the addition of 0.8 mmol l^{-1} NADH.

CI NADH:HAAR activity

Activity of the CI flavin group, not involving the membrane part of the enzyme, was assayed as described above, but in 120 mmol l^{-1} KCl, 1 mmol l^{-1} EDTA, 10 mmol l^{-1} Hepes, pH 7.2, and using 2 mmol l^{-1} hexaammineruthenium(III) chloride (HAAR) as electron acceptor. This assay measures activity of the flavin site at the matrix arm of CI, which is independent of the membrane part of the enzyme.

Citrate synthase activity

All complex activities were standardised to citrate synthase activity, used to approximate mitochondrial content of each species. Citrate synthase activity was assayed as the formation of 2-nitro-5-thiobenzoic acid (TNB) at 412 nm using ε_{TNB} of 13,600 l mol^{-1} cm^{-1} (Srere, 1969). Mitochondrial homogenates were added to 100 mmol l^{-1} Tris, pH 8.0, with 0.1% (v/v) Triton-X-100, 370 µmol l^{-1} acetyl CoA and 100 µmol l^{-1} 5,5′-dithiobis(2-nitrobenzoic acid) (DTNB) and the assay was started by the addition of 66 µmol l^{-1} oxaloacetate.

Respiration rate and H_2O_2 production

Respiration rate and H_2O_2 production of freshly isolated mitochondria were measured in parallel at 25°C in the two chambers of an Oxygraph 2-k high-resolution respirometry system (Oroboros Instruments, Innsbruck, Austria). The system was fitted with an O2k-fluorescence LED2-module with filters for detecting H_2O_2 via the Amplex UltraRed product resorufin. Freshly isolated mitochondria (65 µg protein ml^{-1}) were added to each of the two 2 ml chambers containing respiration buffer (110 mmol l^{-1} sucrose, 20 mmol l^{-1} taurine, 10 mmol l^{-1} KH_2PO_4, 20 mmol l^{-1} Hepes, 60 mmol l^{-1} K-MES, 1.4 mmol l^{-1} $MgCl_2$, 0.5 mmol l^{-1} EGTA, 0.5% BSA, pH 7.4) calibrated with air and Amplex UltraRed assay components (10 µmol l^{-1} Amplex UltraRed, 1 U ml^{-1} horseradish peroxidase, 20 U ml^{-1} superoxide dismutase) and the fluorescence modules were calibrated by injection of 0.1 µmol l^{-1} H_2O_2 in the presence of mitochondria to correct for the endogenous mitochondrial antioxidant capacity (Makrecka-Kuka et al., 2015).

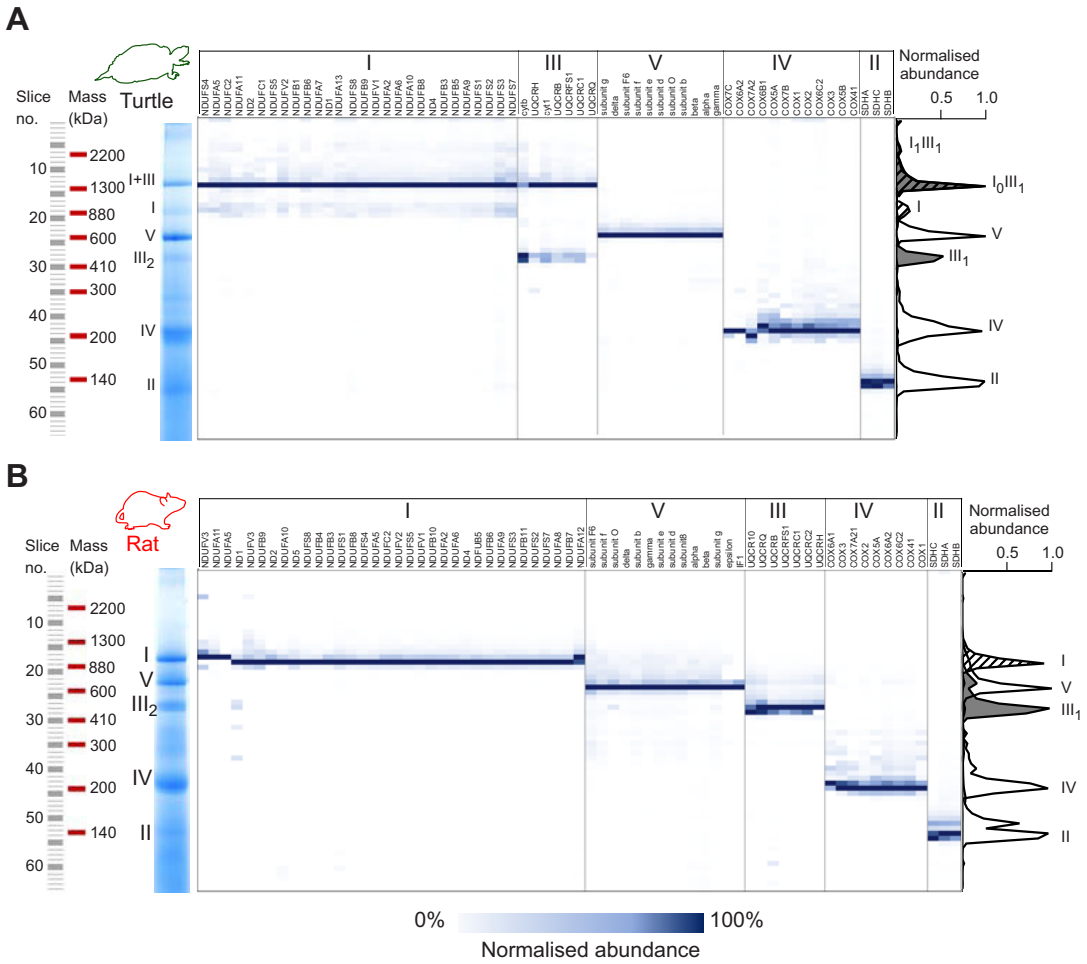

Fig. 2. Protein profiling of ETC complexes. (A) Turtle and (B) rat heart ETC complexes were solubilized with DDM (3.5 g g^{-1} mitochondrial protein) and separated by BN-PAGE. The gel was cut into 64×1 mm slices of equal size and proteins were identified by LC/MS. Normalised protein abundance across the gel lane of each detected subunit was visualised as a heat-map shown in blue. The average abundance of each complex across the gel lane is visualised as an average of the normalised abundance of the subunits for each complex (CI, striated; CII, grey). Note that the maximal abundance of both CI and CIII in turtle mitochondria, in contrast to that of rat, occurs in slice 14 (~1400 kDa).

Journal of Experimental Biology (2020) 223, jeb223776. doi:10.1242/jeb.223776

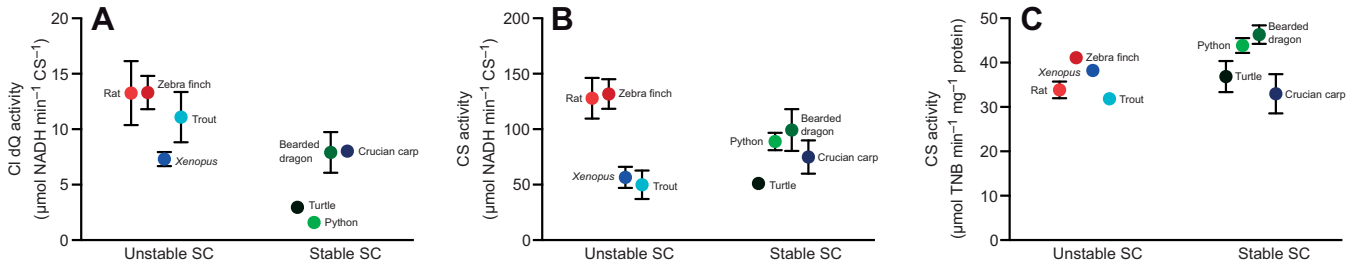

Fig. 3. CI activity of isolated heart mitochondria relative to citrate synthase (CS) activity. CI activity was assessed using (A) decylubiquinone (dQ) or (B) hexaammineruthenium(III) chloride (HAAR) as electron acceptor. (C) CS activity of isolated heart mitochondria. Enzyme activity was measured at 25°C (*N*=5 for all species except trout, *N*=6).

Protocol 1

In one chamber, LEAK (state II, non-phosphorylating) respiration rate was recorded in the presence of 2.5 mmol l^{-1} malate and 5 mmol l^{-1} pyruvate (LEAK MP), before 1 mmol l^{-1} ADP was added to initiate phosphorylating (state III) respiration (P MP). Then, 20 mmol l^{-1} succinate was added (P MPS) to initiate maximal phosphorylating (state III) respiration, and 10 µmol l^{-1} cytochrome *c* (bovine) was injected to test the integrity of the outer mitochondrial membrane. Addition of cytochrome *c* did not increase respiration rate by more than 10% in any experiment. Oligomycin (2.5 µmol l^{-1}) was injected to measure LEAK respiration rate before the mitochondria were uncoupled by sequential additions of FCCP to measure maximal, uncoupled respiration rate. Then, antimycin A (2.5 µmol l^{-1}) was added to measure background oxygen consumption (~50 pmol O_2 s^{-1} mg^{-1} protein), which was subtracted from all measurements. Isolated mitochondria from *P. regius* were insensitive to antimycin A, and so the respiration rate from this species was not corrected for background oxygen consumption.

Protocol 2

In the other chamber, 20 mmol l^{-1} succinate was first added and both respiration rate and maximal H_2O_2 production rate during reverse electron transfer was recorded at [O_2] of ~180 µmol l^{-1}. Then, 8 µg ml^{-1} rotenone was added to eliminate CI-dependent H_2O_2 production, and 1 mmol l^{-1} ADP was added to record phosphorylating respiration rate (P S rot).

Statistics

Data were analysed in Prism 8 (GraphPad software, San Diego, CA, USA) by multiple *t*-tests without assuming similar standard deviations and were corrected for multiple testing using the procedure of Benjamini, Krieger and Yekutieli. All data are shown as means±s.e.m.

RESULTS

To uncover general patterns of SC distribution among vertebrates, we used identical protocols to isolate heart mitochondria from representative species of most vertebrate classes (Fig. 1A). Throughout this study, we standardised mitochondrial isolation, gel electrophoresis protocols, enzyme assays and respiration rate measurements so that they were all conducted under the same conditions, including temperature, to allow meaningful comparisons. The mitochondrial respiratory complexes were resolved by BN-PAGE (Fig. 1B,C). All vertebrates displayed SCs when mitochondria were solubilised with digitonin and in these experiments, CIV activity on the BN-PAGE gel was associated with several large molecular weight bands with CI activity corresponding to SCs (Fig. 1B).

In the presence of DDM, CI and CIII formed a major stable SC (Fig. 1C) in the ectothermic species turtle, bearded dragon, python and crucian carp. The approximate molecular weight estimated from the migration distance on the BN-PAGE of this SC was ~1400 kDa (Fig. 1C), which corresponds to that of a $CICIII_2$ SC (CI 880 kDa+2×CIII 460 kDa=1340 kDa). In the presence of DDM, CIV activity was not associated with any of the SC bands present in ectothermic species, further suggesting that the interaction between $CICIII_2$ and CIV is disrupted in the presence of DDM (Fig. 1C). In contrast, mitochondrial complexes from endothermic species (rat and zebra finch) and *Xenopus* were resolved as separate bands by BN-PAGE, with a single band with CI activity, but no apparent SCs (Fig. 1C). Furthermore, trout mitochondria showed only a very weak

Table 1. Overview of statistics of data presented in Figs 3 and 4

	Unstable SC		Stable SC		
	Mean±s.e.m.	*N*	Mean±s.e.m.	*N*	*P*
Enzyme activity					
Complex I dQ (µmol NADH min^{-1} CS^{-1})	11.3±1.1	21	5.2±0.9	20	<0.001*
Complex I HAAR (µmol NADH min^{-1} CS^{-1})	94.3±12.0	21	79.8±8.0	20	0.326
Citrate synthase (µmol TNB min^{-1} mg^{-1} protein)	36.7±1.2	21	40.2±2.1	20	0.151
Respiration rate					
State II MP (LEAK) (pmol O_2 s^{-1} mg^{-1} protein)	230.3±22.5	21	171.1±27.5	20	0.102
State III MPS (pmol O_2 s^{-1} mg^{-1} protein)	5246.5±587.1	21	3983.3±566.1	20	0.130
FCR (state III/state II)	23.6±3.8	21	24.5±5.8	20	0.896
H_2O_2 production (pmol H_2O_2 s^{-1} mg^{-1} protein)	10.7±1.3	20	7.9±1.7	20	0.199

Animals with unstable supercomplexes (SCs) comprise rat, zebra finch, *Xenopus laevis* (*Xenopus*) and trout; animals with stable SCs comprise turtle, python, bearded dragon and crucian carp. Means were considered significantly different when $P<0.05$, and are marked by an asterisk.
dQ, decylubiquinone; HAAR, hexaammineruthenium(III) chloride; TNB, 2-nitro-5-thiobenzoic acid; MPS, malate+pyruvate+succinate; FCR, flux control ratio; CS, citrate synthase activity.

Journal of Experimental Biology (2020) 223, jeb223776. doi:10.1242/jeb.223776

band corresponding to CI in size with very low in-gel CI activity with both digitonin (Fig. 1B) and DDM (Fig. 1C) and no SC bands.

We then compared the distribution of mitochondrial ETC proteins solubilised with DDM and separated by BN-PAGE from an ectotherm with highly stable SCs (turtle; Fig. 2A) with those from an endotherm with highly unstable SCs (rat; Fig. 2B) by mass-spectrometric protein profiling (complexomics). This analysis conclusively showed that ∼90% of total CI and ∼70% of total CIII from turtle heart mitochondria co-localised on the gel and that the migration distance corresponded to the size of a CI_1CIII_2 SC (1340 kDa) (Fig. 2A). There was also a small (∼5%) co-migration of CI and CIII at a migration position that corresponded to the size of a CI_2CIII_2 SC (2220 kDa) (Fig. 2A). CIV was not associated with either SC band (Fig. 2A), suggesting that CIV is not a stable part of SCs in turtles. In contrast, rat mitochondrial respiratory complexes were completely separated in the presence of DDM and no stable SCs were detected (Fig. 2B). The full distribution of all detected proteins, represented as heat-maps for each species, are available in Table S1. Based on these results, we grouped the species into animals with stable SCs (turtle, python, bearded dragon and crucian carp) and animals with unstable SCs (rat, zebra finch, *Xenopus* and trout). We define stable SC as the presence of a clear band corresponding to the size of $CICIII_2$ and unstable SC as the presence of clearly separated CI and $CIII_2$ bands detected by BN-PAGE with DDM.

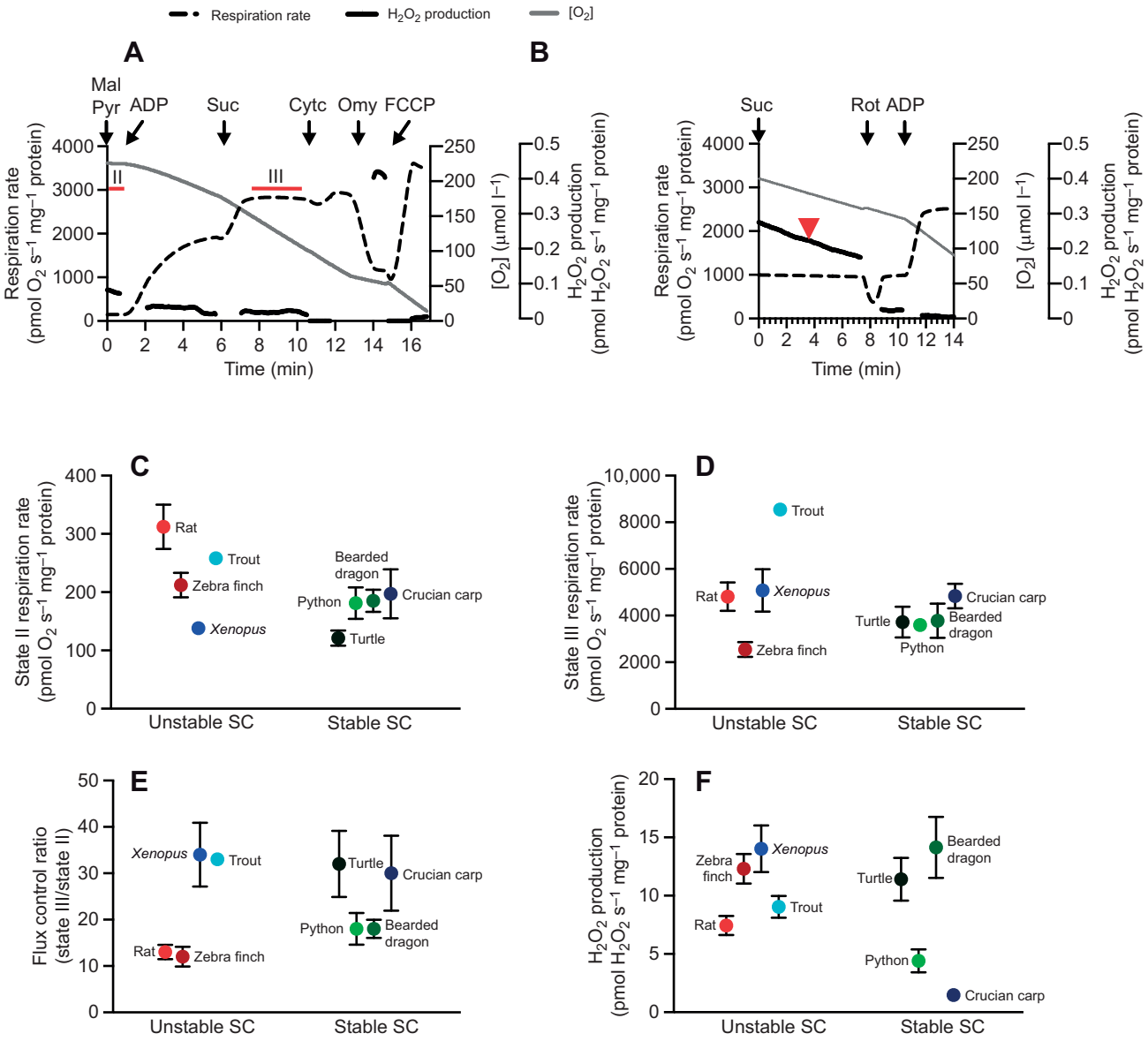

Fig. 4. Respiration rate and reactive oxygen species production in isolated heart mitochondria. (A,B) Representative traces of respiration rate and H_2O_2 production of isolated rat heart mitochondria with (A) protocol 1, where intervals for state II and maximal state III measurements are marked by red bars, and (B) protocol 2, where H_2O_2 production with succinate (reverse electron transfer) was measured at 180 µmol l^{-1} O_2, marked by a red arrowhead. H_2O_2 production rate is shown when traces stabilised after addition of substrates. Mal, malate; Pyr, pyruvate; Suc, succinate; Cytc, cytochrome *c*; Omy, oligomycin; Rot, rotenone. (C) State II respiration rate of isolated heart mitochondria with CI substrates (malate and pyruvate, without ADP) and (D) maximal phosphorylating state III respiration rate with both CI and CII substrates (malate, pyruvate and succinate with ADP), both measured by protocol 1. (E) Flux control ratio of maximal phosphorylating state III respiration rate relative to state II respiration rate. (F) Maximal H_2O_2 production under state II conditions (no ADP) with succinate, measured by protocol 2. All measurements were conducted at 25°C (*N*=5 for all species except trout, *N*=6).

It has been suggested that SCs favour effective electron transfer within the mitochondrial ETC. Average CI activity with decylubiquinone, which reflects the enzymatic activity of the entire enzyme, was significantly lower in animals with stable SCs compared with that in animals with unstable SCs (Fig. 3A, Table 1). CI activity with HAAR as electron acceptor, which only assays the flavin site of the enzyme, was not significantly different between animals with stable and unstable SCs (Fig. 3B, Table 1). Thus, assembly into stable $CICIII_2$ SCs affects the activity of the entire CI enzyme but not that of the flavin site. Citrate synthase activity of the isolated mitochondria was similar for all species (Fig. 3C) and was used to normalise complex I activity.

Next, we measured respiration rate and ROS production in isolated heart mitochondria to test whether SC stability was associated with differences in the ability of mitochondria to transfer electrons between CI and CIII. We found that respiration was coupled in mitochondria from all species, and that respiration rate did not increase more than 10% with the addition of cytochrome *c*, suggesting that the standardised isolation protocol worked well for all species used in this study. State II (LEAK) and III (phosphorylating) respiration rates and the flux control ratio (state III/state II) (Fig. 4A–E) and H_2O_2 production (Fig. 4F) of isolated heart mitochondria varied across species, without any obvious pattern of variation with SC stability (Fig. 1) and no significant differences between animal groups with stable or unstable SCs (Table 1).

The species examined covered a wide range of body temperatures (Fig. 5A) (Bartholomew and Tucker, 1963; Casterlin and Reynolds, 1980; Ebersole et al., 2001; Fink et al., 2018; Fobian et al., 2014; Gudjonsson, 1932; Hochachka and Somero, 2002; Matikainen and Vornanen, 1992; Pitman, 1974; Sköld-Chiriac et al., 2015; Taylor et al., 1996; Ultsch, 2006), and SCs were most stable in animals tolerating large variations in body temperature (Fig. 5B).

DISCUSSION

This study shows that $CICIII_2$ is the main SC across all vertebrate groups and that this SC is more stable in ectotherms than in endotherms, as indicated by the effect of the detergent DDM (Fig. 1). We found CIV associated with several mitochondrial membrane proteins including SCs across the vertebrate species investigated here when mitochondrial membranes were solubilised using the gentle detergent digitonin (Fig. 1B). However, the association with CIV was not stable in the presence of DDM (Fig. 1C), suggesting a less stable interaction than that which maintains the $CICIII_2$ SC. This result supports previous studies of mammalian SCs where the structural interaction of CIV with $CICIII_2$ was not well defined (Althoff et al., 2011; Davies et al., 2018; Gu et al., 2016; Letts et al., 2016; Wu et al., 2016) and reports of SCs formed between CI and CIII without CIV (Greggio et al., 2016; Letts et al., 2016; Lopez-Fabuel et al., 2016). Therefore, while this study does not exclude that $CICIII_nCIV_n$ SCs may be present *in vivo* in all animals investigated here, the interaction between $CICIII_2$ and CIV seems to be weaker and could be a non-specific consequence of low-temperature BN-PAGE with digitonin. As the respective lipid composition and body temperature of each species could also influence the SC associations and this was not investigated in the present study, the true *in vivo* interactions may differ from those described here.

We found that SCs from reptilian species (turtle, python and bearded dragon) were the most stable as they showed a well-defined SC band following BN-PAGE. The pattern of SC distribution was less well defined in endotherms and *Xenopus* and trout, which form unstable SCs (Fig. 1C). Interestingly, trout mitochondria treated with DDM showed no bands with CI activity when resolved by BN-PAGE (Fig. 1C). However, trout mitochondria did show a band with CI activity when treated with digitonin (Fig. 1B). Surprisingly, trout CI activity was similar to that of other ectotherms (Fig. 3) and CI-dependent respiration rate was high in trout mitochondria (Fig. 4), indicating that CI is fully functional in intact mitochondria, although not detected as a single band on the DDM BN-PAGE gel (Fig. 1C).

These results suggest two major groups: poikilothermic ectotherms (crucian carp and the reptiles turtle, python and bearded dragon) with highly stable SCs and homeothermic endotherms (rat and zebra finch) and stenothermic ectotherms (*X. laevis* and trout) with unstable SCs. This grouping suggests that highly stable SCs are a consistent feature of ectothermic (poikilothermic) reptiles and crucian carp which tolerate temperature fluctuations in their environment without needing to regulate body temperature (Fig. 5). Conversely, the unstable nature of trout CI may reflect the stenothermal nature of their temperature tolerance, suggesting that their SC stability is optimised to a narrow thermal window, similar to homeothermic endotherms (Fig. 5). Thus, the requirement for stable SCs that can withstand temperature fluctuations may have been lost separately upon the evolution of endothermy in mammals and birds. It may be that in

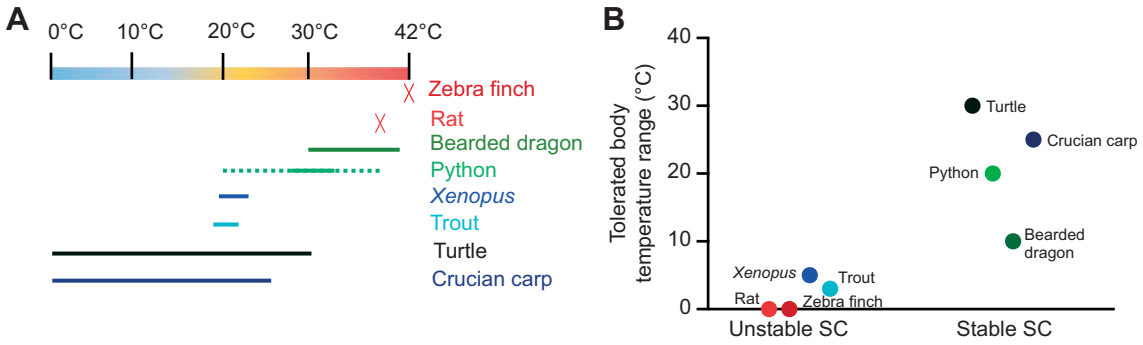

Fig. 5. Body temperature of the study species. (A) Temperature range of the species used: Wistar rat, *Rattus norvegicus* (Gudjonsson, 1932); zebra finch, *Taeniopygia guttata* (Sköld-Chiriac et al., 2015); red-eared slider turtle, *Trachemys scripta elegans* (Ultsch, 2006); ball python, *Python regius*; bearded dragon *Pogona vitticeps* (Bartholomew and Tucker, 1963); African clawed frog, *Xenopus laevis*; crucian carp, *Carassius carassius* (Matikainen and Vornanen, 1992); and rainbow trout, *Oncorhynchus mykiss* (Ebersole et al., 2001; Taylor et al., 1996). The temperature range of *P. regius* was estimated from the maximal and minimal temperatures of their ecological habitat in western sub-Saharan Africa (dotted line) (Pitman, 1974) and the preferred body temperature of other python species (solid line) (Fobian et al., 2014). *Xenopus*' preferred body temperature is 22°C (Casterlin and Reynolds, 1980). (B) Variation in body temperature range in species with unstable and stable SCs.

mammals and birds, endothermy allowed the evolution of other desirable traits. Further studies are required to elucidate these aspects.

It has been argued that the close association between CI and CIII in SCs should enhance electron transfer and increase respiration rates, as well as reduce production of $O_2^{\cdot-}$ and H_2O_2 (Greggio et al., 2016; Lapuente-Brun et al., 2013; Letts and Sazanov, 2017; Lopez-Fabuel et al., 2016; Sousa et al., 2016). However, our data show that state II (LEAK) and III (phosphorylating) respiration rates, the flux control ratio between state III and II as well as H_2O_2 production of isolated heart mitochondria varied across species (Fig. 4), without any obvious pattern of variation with SC stability (Fig. 1). For example, maximal H_2O_2 production under LEAK conditions with succinate was almost identical in zebra finch and turtle mitochondria (Fig. 4F), with unstable and stable SCs (Fig. 1), respectively. Although the intrinsic specific activities of SCs may vary across species, our data suggest that highly stable SCs do not necessarily prevent mitochondrial H_2O_2 production. This result is in agreement with previous results from turtle mitochondria showing that turtle mitochondria produce H_2O_2 at a similar rate to mitochondria from mice (Bundgaard et al., 2019).

Together, the data presented here show that vertebrates can possess either stable or unstable mitochondrial SCs. The major SC detected was of type $CICIII_2$ (without CIV) and it was most stable in poikilothermic ectotherms such as reptiles and crucian carp. In contrast, the low SC stability found within homeothermic endotherms as well as trout and *Xenopus* may reflect the lack of body temperature fluctuations (Fig. 5). This suggests that the stability of SCs is adapted to the lifestyle of a given species and further illustrates that studying SCs from a range of vertebrates may serve as an important tool to gain insight into the overall functional role of SCs.

Acknowledgements
The authors would like to thank Ian Fearnley and Shujing Ding from the University of Cambridge for assistance with mass spectrometry.

Competing interests
The authors declare no competing or financial interests.

Author contributions
Conceptualization: A.B., J.M.A., A.F.; Methodology: A.B., J.M.A., M.E.H., M.P.M., A.F.; Software: M.E.H.; Validation: M.E.H.; Formal analysis: A.B., M.E.H.; Investigation: A.B., J.M.A., M.E.H.; Resources: M.P.M.; Data curation: A.B., M.E.H.; Writing - original draft: A.B.; Writing - review & editing: A.B., J.M.A., M.E.H., M.P.M., A.F.; Visualization: A.B.; Supervision: J.M.A., M.P.M., A.F.; Project administration: J.M.A., M.P.M., A.F.; Funding acquisition: M.P.M., A.F.

Funding
We thank the Aarhus Universitets Forskningsfond (NOVA grant AUFF-E-2016-9-37 to A.F.), the Medical Research Council UK (MC_U105663142 to M.P.M.) and the Wellcome Trust (Investigator award 110159/Z/15/Z to M.P.M.) for support.
Deposited in PMC for release after 6 months.

Supplementary information
Supplementary information available online at
http://jeb.biologists.org/lookup/doi/10.1242/jeb.223776.supplemental

References
Acín-Pérez, R., Fernández-Silva, P., Peleato, M. L., Pérez-Martos, A. and Enriquez, J. A. (2008). Respiratory active mitochondrial supercomplexes. *Mol. Cell* **32**, 529-539. doi:10.1016/j.molcel.2008.10.021

Althoff, T., Mills, D. J., Popot, J.-L. and Kühlbrandt, W. (2011). Arrangement of electron transport chain components in bovine mitochondrial supercomplex $I_1III_2IV_1$. *EMBO J.* **30**, 4652-4664. doi:10.1038/emboj.2011.324

Bartholomew, G. A. and Tucker, V. A. (1963). Control of changes in body temperature, metabolism, and circulation by the agamid. *Physiol. Zool.* **36**, 199-218. doi:10.1086/physzool.36.3.30152307

Bennett, A. F. and Ruben, J. A. (1979). Endothermy and activity in vertebrates. *Science (80–.)* **206**, 649-654. doi:10.1126/science.493968

Blaza, J. N., Serreli, R., Jones, A. J. Y., Mohammed, K. and Hirst, J. (2014). Kinetic evidence against partitioning of the ubiquinone pool and the catalytic relevance of respiratory-chain supercomplexes. *Proc. Natl. Acad. Sci. USA* **111**, 15735-15740. doi:10.1073/pnas.1413855111

Böttinger, L., Horvath, S. E., Kleinschroth, T., Hunte, C., Daum, G., Pfanner, N. and Becker, T. (2012). Phosphatidylethanolamine and cardiolipin differentially affect the stability of mitochondrial respiratory chain supercomplexes. *J. Mol. Biol.* **423**, 677-686. doi:10.1016/j.jmb.2012.09.001

Brand, M. D., Couture, P., Else, P. L., Withers, K. W. and Hulbert, A. J. (1991). Evolution of energy-metabolism - Proton permeability of the inner membrane of liver-mitochondria is greater in a mammal than in a reptile. *Biochem. J.* **275**, 81-86. doi:10.1042/bj2750081

Brookes, P. S., Buckingham, J. A., Tenreiro, A. M., Hulbert, A. and Brand, M. D. (1998). The proton permeability of the inner membrane of liver mitochondria from ectothermic and endothermic vertebrates and from obese rats: correlations with standard metabolic rate and phospholipid fatty acid composition. *Comp. Biochem. Physiol. Part B Biochem. Mol. Biol.* **119**, 325-334. doi:10.1016/S0305-0491(97)00357-X

Bultema, J. B., Braun, H. P., Boekema, E. J. and Kouřil, R. (2009). Megacomplex organization of the oxidative phosphorylation system by structural analysis of respiratory supercomplexes from potato. *Biochim. Biophys. Acta Bioenerg.* **1787**, 60-67. doi:10.1016/j.bbabio.2008.10.010

Bundgaard, A., James, A. M., Joyce, W., Murphy, M. P. and Fago, A. (2018). Suppression of reactive oxygen species generation in heart mitochondria from anoxic turtles: the role of complex I S-nitrosation. *J. Exp. Biol.* **221**, jeb174391. doi:10.1242/jeb.174391

Bundgaard, A., James, A. M., Gruszczyk, A. V., Martin, J., Murphy, M. P. and Fago, A. (2019). Metabolic adaptations during extreme anoxia in the turtle heart and their implications for ischemia-reperfusion injury. *Sci. Rep.* **9**, 2850. doi:10.1038/s41598-019-39836-5

Casterlin, M. E. and Reynolds, W. W. (1980). Diel activity and thermoregulatory behavior of a fully aquatic frog: Xenopus laevis. *Hydrobiologia* **75**, 189-191. doi:10.1007/BF00007433

Davies, K. M., Strauss, M., Daum, B., Kief, J. H., Osiewacz, H. D., Rycovska, A., Zickermann, V. and Kühlbrandt, W. (2011). Macromolecular organization of ATP synthase and complex I in whole mitochondria. *Proc. Natl. Acad. Sci. USA* **108**, 14121-14126. doi:10.1073/pnas.1103621108

Davies, K. M., Blum, T. B., Kühlbrandt, W. and Henderson, R. (2018). Conserved *in situ* arrangement of complex I and III_2 in mitochondrial respiratory chain supercomplexes of mammals, yeast, and plants. *Proc. Natl. Acad. Sci. USA* **115**, 3024-3029. doi:10.1073/pnas.1720702115

Ebersole, J. L., Liss, W. J. and Frissell, C. A. (2001). Relationship between stream temperature, thermal refugia and rainbow trout Oncorhynchus mykiss abundance in arid-land streams in the northwestern United States. *Ecol. Freshw. Fish* **10**, 1-10. doi:10.1034/j.1600-0633.2001.100101.x

Else, P. L. and Hulbert, A. J. (1981). Comparison of the "mammal machine" and the "reptile machine": energy production. *Am. J. Physiol. Regul. Integr. Comp. Physiol.* **240**, R3-R9. doi:10.1152/ajpregu.1981.240.1.R3

Estornell, E., Fato, R., Pallotti, F. and Lenaz, G. (1993). Assay conditions for the mitochondrial NADH:coenzyme Q oxidoreductase. *FEBS Lett.* **332**, 127-131. doi:10.1016/0014-5793(93)80498-J

Eubel, H., Heinemeyer, J., Sunderhaus, S. and Braun, H.-P. (2004). Respiratory chain supercomplexes in plant mitochondria. *Plant Physiol. Biochem.* **42**, 937-942. doi:10.1016/j.plaphy.2004.09.010

Fink, B. D., Bai, F., Yu, L., Sheldon, R. D., Sharma, A., Taylor, E. B. and Sivitz, W. I. (2018). Oxaloacetic acid mediates ADP-dependent inhibition of mitochondrial complex II-driven respiration. *J. Biol. Chem.* **293**, 19932-19941. doi:10.1074/jbc.RA118.005144

Fobian, D., Overgaard, J. and Wang, T. (2014). Oxygen transport is not compromised at high temperature in pythons. *J. Exp. Biol.* **217**, 3958-3961. doi:10.1242/jeb.105148

Genova, M. L. and Lenaz, G. (2014). Functional role of mitochondrial respiratory supercomplexes. *Biochim. Biophys. Acta* **1837**, 427-443. doi:10.1016/j.bbabio.2013.11.002

Genova, M. L., Baracca, A., Biondi, A., Casalena, G., Faccioli, M., Falasca, A. I., Formiggini, G., Sgarbi, G., Solaini, G. and Lenaz, G. (2008). Is supercomplex organization of the respiratory chain required for optimal electron transfer activity? *Biochim. Biophys. Acta Bioenerg.* **1777**, 740-746. doi:10.1016/j.bbabio.2008.04.007

Gong, H., Li, J., Xu, A., Tang, Y., Ji, W., Gao, R., Wang, S., Yu, L., Tian, C., Li, J., et al. (2018). An electron transfer path connects subunits of a mycobacterial respiratory supercomplex. *Science* **362**, eaat8923. doi:10.1126/science.aat8923

Green, R. E., Braun, E. L., Armstrong, J., Earl, D., Nguyen, N., Hickey, G., Vandewege, M. W., St John, J. A., Capella-Gutiérrez, S., Castoe, T. A., et al. (2014). Three crocodilian genomes reveal ancestral patterns of evolution among archosaurs. *Science* **346**, 1254449. doi:10.1126/science.1254449

Greggio, C., Jha, P., Kulkarni, S. S., Lagarrigue, S., Broskey, N. T., Boutant, M., Wang, X., Conde Alonso, S., Ofori, E., Auwerx, J., et al. (2016). Enhanced respiratory chain supercomplex formation in response to exercise in human skeletal muscle. *Cell Metab.* **25**, 444-450. doi:10.1016/j.cmet.2016.11.004

Gu, J., Wu, M., Guo, R., Yan, K., Lei, J., Gao, N. and Yang, M. (2016). The architecture of the mammalian respirasome. *Nature* **537**, 639-643. doi:10.1038/nature19359

Gudjonsson, S. V. (1932). The body temperature in rats on normal and deficient diets: preliminary report. *J. Physiol.* **74**, 73-80. doi:10.1113/jphysiol.1932.sp002830

Guo, R., Zong, S., Wu, M., Yang, M., Gu, J. and Yang, M. (2017). Architecture of human mitochondrial respiratory megacomplex I2III2IV2. *Cell* **170**, 1247-1257.e12. doi:10.1016/j.cell.2017.07.050

Heide, H., Bleier, L., Steger, M., Ackermann, J., Dröse, S., Schwamb, B., Zörnig, M., Reichert, A. S., Koch, I., Wittig, I., et al. (2012). Complexome profiling identifies TMEM126B as a component of the mitochondrial complex I assembly complex. *Cell Metab.* **16**, 538-549. doi:10.1016/j.cmet.2012.08.009

Hoch, F. L. (1992). Cardiolipins and biomembrane function. *Biochim. Biophys. Acta Rev. Biomembr.* **1113**, 71-133. doi:10.1016/0304-4157(92)90035-9

Hochachka, P. W. and Somero, G. N. (2002). *Biochemical Adaptations*. Oxford: Oxford University Press.

Hulbert, A. J. and Else, P. L. (1989). Evolution of mammalian endothermic metabolism: mitochondrial activity and cell composition. *Am. J. Physiol. Regul. Integr. Comp. Physiol.* **256**, R63-R69. doi:10.1152/ajpregu.1989.256.1.R63

Kraffe, E., Marty, Y. and Guderley, H. (2007). Changes in mitochondrial oxidative capacities during thermal acclimation of rainbow trout *Oncorhynchus mykiss*: roles of membrane proteins, phospholipids and their fatty acid compositions. *J. Exp. Biol.* **210**, 149-165. doi:10.1242/jeb.02628

Lapuente-Brun, E., Moreno-Loshuertos, R., Acín-Pérez, R., Latorre-Pellicer, A., Colás, C., Balsa, E., Perales-Clemente, E., Quirós, P. M., Calvo, E., Rodríguez-Hernández, M. A., et al. (2013). Supercomplex assembly determines electron flux in the mitochondrial electron transport chain. *Science* **340**, 1567-1570. doi:10.1126/science.1230381

Letts, J. A. and Sazanov, L. A. (2017). Clarifying the supercomplex: the higher-order organization of the mitochondrial electron transport chain. *Nat. Struct. Mol. Biol.* **24**, 800-808. doi:10.1038/nsmb.3460

Letts, J. A., Fiedorczuk, K. and Sazanov, L. A. (2016). The architecture of respiratory supercomplexes. *Nature* **537**, 644-648. doi:10.1038/nature19774

Letts, J. A., Fiedorczuk, K., Degliesposti, G., Skehel, M. and Sazanov, L. A. (2019). Structures of respiratory supercomplex I+III2 reveal functional and conformational crosstalk. *Mol. Cell* **75**, 1131-1146.e6. doi:10.1016/j.molcel.2019.07.022

Lopez-Fabuel, I., Le Douce, J., Logan, A., James, A. M., Bonvento, G., Murphy, M. P., Almeida, A. and Bolaños, J. P. (2016). Complex I assembly into supercomplexes determines differential mitochondrial ROS production in neurons and astrocytes. *Proc. Natl. Acad. Sci. USA* **113**, 13063-13068. doi:10.1073/pnas.1613701113

Makrecka-Kuka, M., Krumschnabel, G. and Gnaiger, E. (2015). High-resolution respirometry for simultaneous measurement of oxygen and hydrogen peroxide fluxes in permeabilized cells, tissue homogenate and isolated mitochondria. *Biomolecules* **5**, 1319-1338. doi:10.3390/biom5031319

Maranzana, E., Barbero, G., Falasca, A. I., Lenaz, G. and Genova, M. L. (2013). Mitochondrial respiratory supercomplex association limits production of reactive oxygen species from complex I. *Antioxid. Redox Signal.* **19**, 1469-1480. doi:10.1089/ars.2012.4845

Matikainen, N. and Vornanen, M. (1992). Effect of season and temperature acclimation on the function of crucian carp (Carassius Carassius) heart. *J. Exp. Biol.* **167**.

Milenkovic, D., Blaza, J. N., Larsson, N.-G. and Hirst, J. (2017). The enigma of the respiratory chain supercomplex. *Cell Metab.* **25**, 765-776. doi:10.1016/j.cmet.2017.03.009

Mileykovskaya, E. and Dowhan, W. (2009). Cardiolipin membrane domains in prokaryotes and eukaryotes. *Biochim. Biophys. Acta Biomembr.* **1788**, 2084-2091. doi:10.1016/j.bbamem.2009.04.003

Mileykovskaya, E. and Dowhan, W. (2014). Cardiolipin-dependent formation of mitochondrial respiratory supercomplexes. *Chem. Phys. Lipids* **179**, 42-48. doi:10.1016/j.chemphyslip.2013.10.012

Moreno-Lastres, D., Fontanesi, F., García-Consuegra, I., Martín, M. A., Arenas, J., Barrientos, A. and Ugalde, C. (2012). Mitochondrial complex I plays an essential role in human respirasome assembly. *Cell Metab.* **15**, 324-335. doi:10.1016/j.cmet.2012.01.015

Paradies, G., Paradies, V., De Benedictis, V., Ruggiero, F. M. and Petrosillo, G. (2014). *Functional Role of Cardiolipin in Mitochondrial Bioenergetics*. Elsevier.

Pfeiffer, K., Gohil, V., Stuart, R. A., Hunte, C., Brandt, U., Greenberg, M. L. and Schägger, H. (2003). Cardiolipin stabilizes respiratory chain supercomplexes. *J. Biol. Chem.* **278**, 52873-52880. doi:10.1074/jbc.M308366200

Pitman, C. R. S. (1974). *Guide to the Snakes of Uganda*. Wheldon & Wesley.

Ruben, J. (1995). The evolution of endothermy in mammals and birds: from physiology to fossils. *Annu. Rev. Physiol,* **57**, 69-95. doi:10.1146/annurev.ph.57.030195.000441

Schägger, H. and Pfeiffer, K. (2001). The ratio of oxidative phosphorylation complexes I–V in bovine heart mitochondria and the composition of respiratory chain supercomplexes. *J. Biol. Chem.* **276**, 37861-37867.

Schägger, H., Pfeiffer, K., Anemüller, S., Lübben, M., Schäfer, G., Arnold, I., Pfeiffer, K., Neupert, W., Stuart, R., Schägger, H., et al. (2000). Supercomplexes in the respiratory chains of yeast and mammalian mitochondria. *EMBO J.* **19**, 1777-1783. doi:10.1093/emboj/19.8.1777

Schägger, H., de Coo, R., Bauer, M. F., Hofmann, S., Godinot, C. and Brandt, U. (2004). Significance of respirasomes for the assembly/stability of human respiratory chain complex I. *J. Biol. Chem.* **279**, 36349-36353. doi:10.1074/jbc.M404033200

Senkler, J., Rugen, N., Eubel, H., Hegermann, J. and Braun, H.-P. (2018). Absence of complex I implicates rearrangement of the respiratory chain in european mistletoe. *Curr. Biol.* **28**, 1606-1613.e4. doi:10.1016/j.cub.2018.03.050

Shimada, S., Oosaki, M., Takahashi, R., Uene, S., Yanagisawa, S., Tsukihara, T. and Shinzawa-Itoh, K. (2018). A unique respiratory adaptation in Drosophila independent of supercomplex formation. *Biochim. Biophys. Acta Bioenerg.* **1859**, 154-163. doi:10.1016/j.bbabio.2017.11.007

Sköld-Chiriac, S., Nord, A., Tobler, M., Nilsson, J-Å and Hasselquist, D. (2015). Body temperature changes during simulated bacterial infection in a songbird: fever at night and hypothermia during the day. *J. Exp. Biol.* **218**, 2961-2969. doi:10.1242/jeb.122150

Sousa, J. S., Mills, D. J., Vonck, J. and Kü hlbrandt, W. (2016). Functional asymmetry and electron flow in the bovine respirasome. *Elife* **5**, e21290. doi:10.7554/eLife.21290

Srere, P. A. (1969). Citrate synthase. *Methods Enzymol.* **13**, 3-11. doi:10.1016/0076-6879(69)13005-0

Stroh, A., Anderka, O., Pfeiffer, K., Yagi, T., Finel, M., Ludwig, B. and Schägger, H. (2004). Assembly of respiratory complexes I, III, and IV into NADH oxidase supercomplex stabilizes complex I in Paracoccus denitrificans. *J. Biol. Chem.* **279**, 5000-5007. doi:10.1074/jbc.M309505200

Taylor, S., Egginton, S. and Taylor, E. (1996). Seasonal temperature acclimatisation of rainbow trout: cardiovascular and morphometric influences on maximal sustainable exercise level. *J. Exp. Biol.* **199**, 835-845.

Trounce, I. A., Kim, Y. L., Jun, A. S. and Wallace, D. C. (1996). Assessment of mitochondrial oxidative phosphorylation in patient muscle biopsies, lymphoblasts, and transmitochondrial cell lines. *Methods Enzymol.* **264**, 484-509. doi:10.1016/S0076-6879(96)64044-0

Ultsch, G. R. (2006). The ecology of overwintering among turtles: where turtles overwinter and its consequences. *Biol. Rev. Camb. Philos. Soc.* **81**, 339-367. doi:10.1017/S1464793106007032

Wodtke, E. (1981). Temperature adaptation of biological membranes. The effects of acclimation temperature on the unsaturation of the main neutral and charged phospholipids in mitochondrial membranes of the carp (*Cyprinus carpio* L.). *Biochim. Biophys. Acta Biomembr.* **640**, 698-709. doi:10.1016/0005-2736(81)90100-0

Wu, M., Gu, J., Guo, R., Huang, Y., Yang, M., Acín-Pérez, R., Bayona-Bafaluy, M. P., Fernández-Silva, P., Moreno-Loshuertos, R., Pérez-Martos, A., et al. (2016). Structure of mammalian respiratory supercomplex $I_1III_2IV_1$. *Cell* **167**, 1598-1609.e10. doi:10.1016/j.cell.2016.11.012

Zhang, M., Mileykovskaya, E. and Dowhan, W. (2002). Gluing the respiratory chain together: Cardiolipin is required for supercomplex formation in the inner mitochondrial membrane. *J. Biol. Chem.* **277**, 43553-43556. doi:10.1074/jbc.C200551200